

Hydrophobic Contributions to the Membrane Docking of Synaptotagmin 7 C2A Domain: Mechanistic Contrast between Isoforms 1 and 7

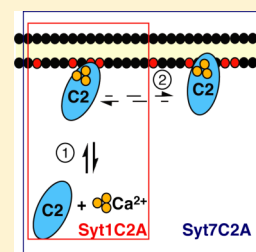
Devin S. Brandt,^{†,‡,§,⊥} Matthew D. Coffman,^{‡,⊥} Joseph J. Falke,[‡] and Jefferson D. Knight^{*,†,‡}

[†]Molecular Biophysics Program and Department of Chemistry and Biochemistry, University of Colorado Boulder, Campus Box 596, Boulder, Colorado 80309, United States

[‡]Department of Chemistry, University of Colorado Denver, Campus Box 194, P.O. Box 173364, Denver, Colorado 80217, United States

S Supporting Information

ABSTRACT: Synaptotagmin (Syt) triggers Ca^{2+} -dependent membrane fusion via its tandem C2 domains, C2A and C2B. The 17 known human isoforms are active in different secretory cell types, including neurons (Syt1 and others) and pancreatic β cells (Syt7 and others). Here, quantitative fluorescence measurements reveal notable differences in the membrane docking mechanisms of Syt1 C2A and Syt7 C2A to vesicles comprised of physiological lipid mixtures. In agreement with previous studies, the Ca^{2+} sensitivity of membrane binding is much higher for Syt7 C2A. We report here for the first time that this increased sensitivity is due to the slower target membrane dissociation of Syt7 C2A. Association and dissociation rate constants for Syt7 C2A are found to be ~ 2 -fold and ~ 60 -fold slower than Syt1 C2A, respectively. Furthermore, the membrane dissociation of Syt7 C2A but not Syt1 C2A is slowed by Na_2SO_4 and trehalose, solutes that enhance the hydrophobic effect. Overall, the simplest model consistent with these findings proposes that Syt7 C2A first docks electrostatically to the target membrane surface and then inserts into the bilayer via a slow hydrophobic mechanism. In contrast, the membrane docking of Syt1 C2A is known to be predominantly electrostatic. Thus, these two highly homologous domains exhibit distinct mechanisms of membrane binding correlated with their known differences in function.



Membrane-targeting C2 domains are central components of many cellular signaling pathways, including secretion, chemotaxis, and cell growth.^{1–3} Initially identified as homologues of the second conserved domain of protein kinase C (PKC), over 400 C2 domains have been identified in human proteins to date.^{4,5} One major function of C2 domains is targeting membrane surfaces upon binding one or more Ca^{2+} ions.^{2,3,6} This activity drives Ca^{2+} -sensitive membrane docking of soluble parent proteins (e.g., conventional PKCs) or drives additional membrane docking for proteins already tethered to a membrane [e.g., synaptotagmins (Syt)].

C2 domains are known to dock to their target membranes via various combinations of electrostatic and hydrophobic interactions. For example, the C2 domain from protein kinase Ca (PKC α C2) binds to anionic headgroups of phosphatidylserine (PS) and phosphatidylinositol-(4,5)-bisphosphate [$\text{PI}(4,5)\text{P}_2$, PIP_2], while the C2 domain from cytosolic phospholipase A_2 (cPLA $_2$ C2) penetrates deeply into the hydrocarbon core of phosphatidylcholine (PC)-rich membranes.^{7–9} This difference in target lipid specificity yields the observed difference in intracellular targeting; PKC α is targeted to plasma membrane while cPLA $_2$ translocates to internal membranes during a Ca^{2+} signaling event.^{7,8,10,11} Deeply inserting C2 domains such as cPLA $_2$ C2 typically exhibit slower membrane association and dissociation rates than domains that interact mainly with headgroups, such as PKC β C2 or the first C2 domain from synaptotagmin 1 (Syt1

C2A).^{9,12,13} Among C2 domains that target anionic lipid headgroups, some have been observed to specifically recognize PIP_2 in addition to the more abundant PS (e.g., PKC α C2 and Syt1 C2B),^{8,11,14,15} while others appear to use less specific electrostatic interactions (e.g., Syt1 C2A).^{16,17}

Syt family proteins serve as Ca^{2+} -sensitive triggers for membrane fusion in secretory cells.^{18–20} Seventeen human isoforms are known, each of which contains two C2 domains (C2A and C2B) and an N-terminal transmembrane helix.^{21–23} Of the known isoforms, Syt1 is by far the most widely studied and is well-known to localize to neurosecretory vesicles.^{19,21} Syt1 plays a central role in rapid neurotransmitter secretion, and other isoforms including Syt2 and Syt9 are also involved in this process.^{17,21}

Other cell types use Syt isoforms for secretion in processes that involve lower peak Ca^{2+} signals and slower response times than neurons. For example, Syt7 is the primary isoform responsible for Ca^{2+} -triggered insulin secretion by the β cells of the pancreas, while Syt1 and Syt2 are not detected in primary β cells.^{21,24} The N-terminal helix of Syt7 is anchored predominantly to insulin secretory vesicles in β cells, although it has been observed in other intracellular locations depending on

Received: May 30, 2012

Revised: September 1, 2012

Published: September 11, 2012

Table 1. Physiological Target Membrane Lipid Compositions (%)

membrane	PC	PS	PE	PI	PG	CH	SM	PIP ₂	dansylPE
TM(−)PIP ₂	10.7	21.3	27.9	5.6	0	25	4.5	0	5
TM(+)PIP ₂	10.7	21.3	27.9	4.6	0	25	4.5	1	5
TM[11% PS]	10.7	11.3	37.9	5.6	0	25	4.5	0	5
TM[31% PS]	10.7	31.3	17.9	5.6	0	25	4.5	0	5
TM(−)PS/PI(+)PG	10.7	0	27.9	0	26.9	25	4.5	0	5

expression level and cell type.^{24,25,26} Syt7 is also found in lysosomal membranes of macrophages, where it is suggested to play a role in their exocytosis.²⁷

Homologous C2 domains from within the same protein family (e.g., PKC C2 domains or Syt C2A domains) have been reported to exhibit differences in membrane binding, such as altered Ca²⁺ binding cooperativity and affinity, that tune different isoforms for their distinct functional and cellular contexts.^{28,29} C2A domains of Syt isoforms are known to vary in Ca²⁺ sensitivity of membrane binding, with Syt7 C2A being one of the most Ca²⁺-sensitive.²⁹ Despite known differences in Ca²⁺-triggered membrane binding *affinity*, C2 domains of the same protein family typically exhibit the same binding *mechanism*.

Here, we report significant differences in the Ca²⁺-dependent membrane binding reactions of C2A domains from Syt1 and Syt7. In contrast to the rapid membrane association and dissociation rates characteristic of Syt1 C2A, the corresponding domain from Syt7 displays slow kinetics reminiscent of those of cPLA₂ C2.^{7,12} Solute sensitivities of dissociation kinetics are consistent with a significant role of the hydrophobic effect for Syt7 C2A membrane interaction. The simplest interpretation is that membrane-bound Syt7 C2A possesses stronger hydrophobic interactions with the bilayer than Syt1 C2A, although other explanations cannot yet be ruled out. On the basis of these results, we propose a two-state docking model for Syt7 C2A, wherein the domain initially binds the membrane surface via electrostatic interactions and is subsequently stabilized by hydrophobic insertion.

MATERIALS AND METHODS

Materials. All lipids were synthetic unless otherwise indicated. Cholesterol (CH), 1-palmitoyl-2-oleoyl-*sn*-glycero-3-phosphocholine (phosphatidylcholine, PC), 1-palmitoyl-2-oleoyl-*sn*-glycero-3-phosphoethanolamine (phosphatidylethanolamine, PE); phosphatidylinositol (PI) natural from bovine liver, 1-palmitoyl-2-oleoyl-*sn*-glycero-3-phosphoserine (phosphatidylserine, PS), 1-palmitoyl-2-oleoyl-*sn*-glycero-3-phospho-(1'-*rac*-glycerol) (phosphatidylglycerol, PG), sphingomyelin (SM) natural from brain, and phosphatidylinositol-4,5-bisphosphate [PI(4,5)P₂, PIP₂] natural from brain were from Avanti. *N*-[5-(Dimethylamino)naphthalene-1-sulfonyl]-1,2-dihexadecanoyl-*sn*-glycero-3-phosphoethanolamine (dansyl-PE, dPE) was from Invitrogen. Other chemicals were of high-quality USP or analytical grade.

Cloning, Protein Expression, and Purification. Human Syt7 DNA was obtained from American Type Culture Collection (clone 11045721). The C2A domain (residues N135–S266, based on numbering in GenBank AAI25171) was PCR-amplified and subcloned into a GST expression vector developed previously by the Falke laboratory.³⁰ Fusion protein was expressed in *E. coli* and purified using a glutathione affinity column, including extensive washing with 0.5 M NaCl to remove any nonspecifically bound nucleic acids prior to

cleavage with thrombin and elution of the free C2 domain. cPLA₂ C2, PKCα C2, and rat Syt1 C2A were also expressed as GST fusions, as described previously, and purified by the same method.^{7,12} The cPLA₂ C2 domain was further purified by Ca²⁺-dependent binding to PC-phenyl sepharose resin, followed by elution with ethylenediaminetetraacetic acid (EDTA).³¹ Proteins were stored in Buffer A [140 mM KCl, 15 mM NaCl, 25 mM *N*-(2-hydroxyethyl)piperazine-*N*-2-ethanesulfonic acid (HEPES), pH 7.4]. Any residual nucleic acid contamination (assessed by absorbance at 260 nm) was removed by benzonase treatment followed by extensive buffer exchange in a centrifugal concentrator. Protein purity was ≥95% as determined by SDS-PAGE, identity was verified using mass spectrometry, and concentration was determined by absorbance at 280 nm in 5 M guanidinium HCl.

Preparation of Lipid Mixtures and Phospholipid Vesicles. Lipids in chloroform were mixed at the desired molar ratios, dried under a stream of nitrogen, and then further dried under vacuum for 2 h. The dried lipids were then hydrated with Buffer A. Small unilamellar phospholipid vesicles were generated by sonicating the hydrated lipids to clarity with a Misonix XL2020 probe sonicator. The vesicle stock solutions used in the equilibrium Ca²⁺ titrations and kinetic experiments were prepared with a total accessible lipid concentration of 1.5 mM with the mole percentages for target membranes given in Table 1.

Steady-State Fluorescence Spectroscopy. Steady-state fluorescence experiments were carried out on a Photon Technology International QM-2000-6SE fluorescence spectrometer at 25 °C. The excitation and emission slit widths were 1 and 8 nm, respectively, for all measurements. All buffers were made with Chelex-treated Ca²⁺-free water. Protein and vesicle stock solutions were incubated with Chelex resin to remove residual Ca²⁺ before use. Quartz cuvettes and stir bars were decalcified by soaking in 50 mM EDTA and rinsing extensively with Ca²⁺-free water prior to use.

Equilibrium Measurement of Ca²⁺-Dependent Protein-to-Membrane FRET. To determine the Ca_{1/2} of each C2 domain, protein–membrane binding assays were performed as described previously.³² Briefly, protein (0.5 μM) was added to vesicles (100 μM total accessible lipid) in a quartz cuvette. CaCl₂ was titrated in to each cuvette, and fluorescence resonance energy transfer (FRET) was measured with 284 nm excitation, 512 nm emission, and 10 s integration. Each intensity value was corrected for dilution, and the intensity of a blank sample was subtracted containing only buffer, lipid, and Ca²⁺. Reversibility was verified following all Ca²⁺ titrations by measuring fluorescence after addition of sufficient EDTA to chelate all free calcium. Data were fit using Kaleidagraph (Synergy Software) to the Hill equation

$$\Delta F = \Delta F_{\max} \frac{[\text{Ca}^{2+}]^H}{[\text{Ca}^{2+}]^H + (\text{Ca}_{1/2})^H} \quad (1)$$

where ΔF is the fluorescence increase, H is the Hill coefficient, and ΔF_{\max} is the calculated maximal fluorescence change. Data in figures are shown following normalization of ΔF_{\max} to unity for each titration, except where noted otherwise.

Equilibrium fluorescence measurements were performed in Buffer A. For a subset of Ca^{2+} titrations, including those for which $\text{Ca}_{1/2} < 3 \mu\text{M}$, a Ca^{2+} buffering system including 1.5 mM nitrilotriacetic acid (NTA) and 1 mM MgCl_2 was used in order to maintain total Ca^{2+} well in excess of protein. In these titrations, the free Ca^{2+} concentration was calculated using MaxChelator. Reliability of this system is demonstrated by measurements with Syt7 C2A on TM(−)PIP₂ in both the presence and absence of this Ca^{2+} buffering system, whose $\text{Ca}_{1/2}$ values differ by <20% (Table 2).

Table 2. Best-Fit Parameters from Equilibrium Calcium Titrations

protein domain	membrane	$\text{Ca}_{1/2}^a$ (μM)	Hill coeff ^a
Syt1 C2A	1:1 PC:PS/5% dPE	31 ± 2	2.4 ± 0.4
Syt1 C2A	TM(−)PIP ₂	43 ± 1	1.8 ± 0.1
Syt1 C2A	TM(+)/PIP ₂	37 ± 1	1.9 ± 0.1
Syt7 C2A	1:1 PC:PS/5% dPE	1.7 ± 0.2^b	2.2 ± 0.1
Syt7 C2A	TM[11% PS]	8 ± 1^b	2.6 ± 0.1
Syt7 C2A	TM(−)PIP ₂	5.4 ± 0.4^b	2.7 ± 0.2
		4.7 ± 0.2	3.4 ± 0.5
Syt7 C2A	TM[31% PS]	2.2 ± 0.1^b	2.0 ± 0.1
Syt7 C2A	TM(+)/PIP ₂	3.4 ± 0.2	2.8 ± 0.4
Syt7 C2A	TM(−)/PS/PI(+)/PG	5.1 ± 0.3^b	3.0 ± 0.1
PKC α C2	TM(−)PIP ₂	30 ± 10	1.0 ± 0.1
PKC α C2	TM(+)/PIP ₂	7.7 ± 0.5	1.9 ± 0.1

^aBest-fit parameters were determined by fitting titration data to the Hill equation (eq 1). The mean and standard deviation of these parameters are reported from at least three independent titrations for each protein–membrane pair. ^bTitration performed in a Ca^{2+} buffering system using NTA (see Materials and Methods).

Equilibrium Measurement of Ionic Strength Dependence of Membrane Binding. C2 domains (0.5 μM) were premixed with TM(−)PIP₂ vesicles (100 μM total accessible lipid) in Buffer A + 1 mM MgCl_2 and excess CaCl_2 . The Ca^{2+} concentrations used were 1 mM for Syt1 C2A and 200 μM for Syt7 C2A, since liposome flocculation was sometimes observed with Syt7 C2A at higher Ca^{2+} concentrations. These Ca^{2+} concentrations are well in excess of $\text{Ca}_{1/2}$, resulting in a maximal FRET efficiency as monitored by dansyl emission at 512 nm. NaCl was titrated into each cuvette, and fluorescence was measured as described above, with a sample lacking protein serving as a blank. A baseline value of fluorescence due to direct dansyl excitation at 284 nm was obtained by adding sufficient EDTA to fully chelate calcium at the end of the titration. This value was subtracted from all measurements, and the corrected initial fluorescence intensity was normalized to unity.

Stopped-Flow Measurement of Association and Dissociation Kinetics. All kinetic experiments were performed on an Applied Photophysics SX.17 stopped-flow fluorescence spectrophotometer at 25 °C in Buffer A, unless otherwise indicated. The dead time of the instrument was 0.9 ± 0.1 ms; thus, all data points prior to 1 ms were eliminated prior to quantitative analysis. The excitation wavelength and slit-width settings on the excitation monochromator were 284 and 6 nm, respectively, and a 475 nm long-pass filter was used for detecting dansyl (acceptor) emission. To determine the

observed rate constant for membrane association (k_{obs}), C2 domains (0.5 μM , all concentrations after mixing) and Ca^{2+} (200 μM) were rapidly mixed with vesicles (100 μM total accessible lipid). The resulting time course exhibited increasing fluorescence intensity with time, which was fit to a single-exponential function:

$$F = \Delta F_{\max}(1 - e^{-k_{\text{obs}}t}) + C \quad (2)$$

where k_{obs} is the apparent association rate constant and C is an offset. To simplify representations, C was subtracted and ΔF_{\max} normalized to unity in figures shown.

To determine the rate constant for the dissociation (k_{off}) of C2 domains from the membranes, the ternary complex of C2 domains (0.5 μM), vesicles (100 μM total accessible lipid), and Ca^{2+} (200 μM) was assembled. The ternary complex was then rapidly mixed with an equal volume of EDTA (1 mM after mixing). The return to equilibrium was monitored using the decrease in dansyl emission as the C2 domain dissociated from the membrane. The data were subjected to nonlinear least-squares fitting to a single- or double-exponential function (eq 3 or 4, respectively):

$$F = \Delta F_{\max}(1 - e^{-k_{\text{off}}t}) + C \quad (3)$$

$$F = \Delta F_{\max 1}(1 - e^{-k_{\text{off}1}t}) + F_{\max 2}(1 - e^{-k_{\text{off}2}t}) + C \quad (4)$$

where the k_{off} are dissociation rate constants and C is an offset. Similarly to association plots, C was subtracted and ΔF_{\max} (or $\Delta F_{\max 1} + \Delta F_{\max 2}$) normalized to unity in figures shown.

Single-Molecule Diffusion Measurement. Protein lateral diffusion was measured using total internal reflection fluorescence (TIRF) microscopy essentially as described previously.^{33,34} C2 domains were engineered to include the 11-amino acid recognition sequence for Sfp phosphopantetheinyltransferase and labeled using this enzyme.^{33,35} Supported lipid bilayers containing a 3:1 mixture of DOPC and DOPS were prepared as described previously.³³ These were imaged in single-molecule imaging buffer (Buffer A with 20 mM 2-mercaptoethanol, 0.5 mM MgCl_2 , and 200 μM CaCl_2) at 20 °C before and after addition of protein. Images were taken on a TIRF microscope with simultaneous excitation at 532 and 640 nm, and the two emission wavelengths were imaged simultaneously from the same view area on different areas of the CCD camera. Particles were tracked using ImageJ and diffusion constants were determined in Mathematica (Wolfram Research) as described previously.³³

RESULTS

Strategy. The goal of this study is to compare the kinetic and equilibrium membrane binding properties of Syt7 C2A to those of the well-studied Syt1 C2A, in order to shed light on the mechanism underlying the known, higher Ca^{2+} sensitivity of Syt7 C2A that is crucial for its signaling function. The domains were expressed in *E. coli* as GST fusions, purified by affinity chromatography, and eluted following thrombin cleavage between the GST and C2 domains. In addition, cPLA₂ C2 and PKC α C2 domains were isolated as previously described for use in control experiments.⁷

In order to best approximate the complexity and negative charge density of the native membranes targeted by these protein domains *in vivo*, except where noted otherwise experiments comparing the two domains were performed with lipid compositions reflecting the content of physiological

target membranes (TM, see Materials and Methods). It is currently debated whether Syt C2A domains target the plasma membrane or secretory vesicle membrane during fusion.^{36–38} Furthermore, the lipid compositions of these two subcellular membranes in β cells have not been reported. However, on the basis of measurements of neuronal secretory vesicle and erythrocyte plasma membrane compositions,^{39,40} and assuming similar asymmetry due to flippase activity,⁴¹ we estimate that the cytosolic faces of these two membranes have similar lipid compositions approximated by the TM membranes used in this study. One notable exception is the polyanionic lipid PI(4,5)P₂, which is found exclusively in the plasma membrane.^{42,43} Thus, our experiments compare C2A binding to membranes both lacking PI(4,5)P₂ [TM(–)PIP₂] and containing 1% PI(4,5)P₂ [TM(+PIP₂)].

Ca²⁺ Dependence of C2A-Membrane Docking. Syt7 C2A has been previously reported to be among the most Ca²⁺-sensitive Syt C2A domains for docking to simple membranes comprised of PC and PS.²⁹ As a functional test of purified protein, the Ca²⁺ sensitivity of membrane binding was measured using a protein-to-membrane FRET assay previously used in our laboratory with Syt1 C2A.^{12,32} Ca²⁺ was titrated into samples containing 0.5 μ M Syt1 C2A or Syt7 C2A domain and excess liposomes (SUVs) containing PC:PS (1:1) with 5% dansyl-PE, and the tryptophan-to-dansyl FRET efficiency was measured as a function of [Ca²⁺] (Figure 1). Fitting of titration

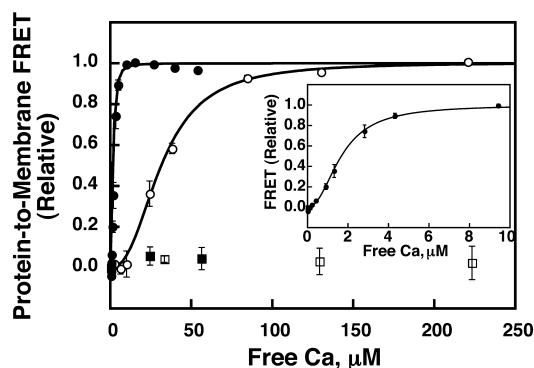


Figure 1. Ca²⁺ sensitivity of membrane binding. CaCl₂ was titrated into 0.5 μ M Syt1 C2A (open symbols) or Syt7 C2A (closed symbols) in the presence of PC:PS(1:1)/5% dPE or PC/3% dPE vesicles (squares), beginning with Ca²⁺-free solutions. Protein-to-membrane FRET was measured as described in Materials and Methods. Points and error bars shown are mean \pm standard deviation of three independent replicate titrations. Data were normalized based on best fits to the Hill equation (solid curves, eq 1); the parameters from these fits are given in Table 2. Data shown are normalized based on these fits. PC control data are normalized to corresponding PC:PS titration data after adjusting for dPE content. Inset shows expansion of the Syt7 C2A binding curve.

curves to the Hill equation yielded Hill cooperativity coefficients and Ca_{1/2} values, defined as the concentration of Ca²⁺ at which membrane binding is half-maximal. The measured Ca_{1/2} values were 31 \pm 2 and 1.7 \pm 0.2 μ M for Syt1 C2A and Syt7 C2A, respectively (Figure 1 and Table 2). Hill coefficients for both domains were greater than 1, as expected for cooperative binding of multiple Ca²⁺ ions by each domain.^{9,14,31} The Ca_{1/2} value of Syt1 C2A is similar to that reported previously in our laboratory using the same lipid composition,¹² and the Ca_{1/2} value of Syt7 C2A is comparable

with a previous report using 3:1 PC:PS and GST-fused protein.²⁹

Syt1 C2A is known to target anionic lipids nonspecifically, with no significant preference for PI(4,5)P₂.¹⁶ Syt7 C2A has been reported to bind PC/1.5%PI(4,5)P₂ membranes in a Ca²⁺-dependent manner, but the effect of PI(4,5)P₂ on its Ca²⁺ sensitivity toward PS-containing membranes has not been tested.⁴⁴ Here, Ca²⁺ titrations were carried out to measure Syt1 C2A and Syt7 C2A docking to physiological target membranes with and without PI(4,5)P₂ [TM(+PIP₂) and TM(–)PIP₂], and the fit parameters are reported in Table 2. Ca_{1/2} values on TM(–)PIP₂ were slightly greater than those on PC:PS (1:1) membranes for both domains, as expected due to the lower density of anionic lipids in TM(–)PIP₂. Addition of PI(4,5)P₂ to generate the TM(+PIP₂) mixture decreased Ca_{1/2} values by less than 30% for both C2A domains. This behavior is clearly distinct from that reported for PKC α C2, whose Ca_{1/2} is strongly dependent on the presence of PI(4,5)P₂.^{7,8,45} As a positive control, a 4-fold Ca_{1/2} decrease was measured in parallel studies of PKC α C2 binding to the same TM(+PIP₂) and TM(–)PIP₂ membranes (Table 2). In other control measurements, FRET was not observed for either C2A domain in the presence of membranes containing only PC and dPE (Figure 1), nor with PS-containing membranes in the absence of Ca²⁺ (Supporting Information Figure S1). Overall, these observations are consistent with both domains having a Ca²⁺-dependent association with anionic lipids but without significant enhancement derived from additional targeting to PI(4,5)P₂.

Electrostatic Contributions to Membrane Docking. In order to directly test for electrostatic contributions to Syt7 C2A membrane interaction, Ca²⁺ titrations were performed with this domain on membranes with varying mole fractions of the anionic lipid PS. Overall, the TM(–)PIP₂ mixture contains 31% anionic lipids (21% PS, 5% PI, and 5% dPE). The measured Ca_{1/2} values increase from 2.2 \pm 0.1 μ M on membranes containing 31% PS to 8 \pm 1 μ M on membranes containing 11% PS, reflecting a large effect of anionic lipid content on apparent membrane affinity (Figure 2 and Table 2). When the PS and PI in the TM mixture are quantitatively substituted with the

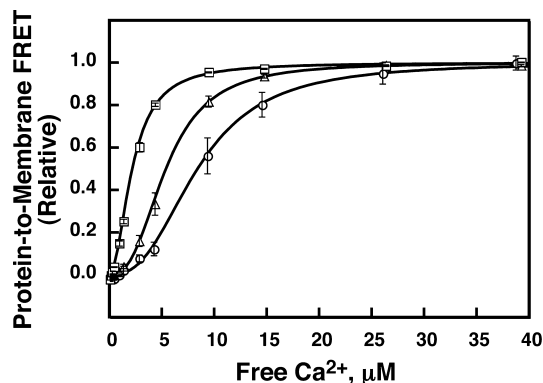


Figure 2. PS sensitivity of Syt7 C2A Ca²⁺/membrane binding. CaCl₂ was titrated into 0.5 μ M Syt7 C2A in the presence of membrane vesicles containing different amounts of the anionic lipid PS (squares: TM[31%PS]; triangles: standard TM(–)PIP₂ containing 21% PS; circles: TM[11%PS]). Points and error bars shown are mean \pm standard deviation of three independent replicate titrations. Data were normalized based on best fits to the Hill equation (solid curves, eq 1); the parameters from these fits are given in Table 2.

anionic lipid phosphatidylglycerol (PG), Syt7 C2A retains Ca^{2+} -dependent membrane binding with a $\text{Ca}_{1/2}$ within error of the standard TM composition [Table 2, TM(-)PS/PI(+PG)]. Clearly, the anionic character of the membrane is a key determinant of Syt7 C2A affinity (Figure 1), reflecting an electrostatic component to the membrane docking interaction similar to that previously reported for Syt1 C2A.¹⁶

To test whether the electrostatic component of membrane interaction is required for Ca^{2+} -triggered Syt7 C2A-membrane docking, NaCl was titrated into C2A/ Ca^{2+} /liposome mixtures up to a final concentration of 700 mM (Figure 3). As judged by

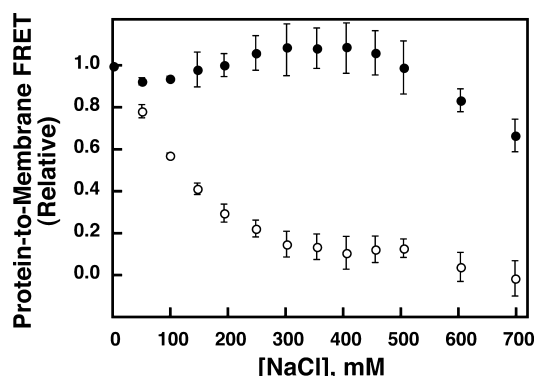


Figure 3. Sensitivity of Syt C2A-membrane interactions to electrostatic screening. Syt1 C2A (0.5 μM , open circles) or Syt7 C2A (0.5 μM , filled circles) was incubated in a fluorescence cell initially in Buffer A containing TM(-)PIP₂ vesicles (100 μM total accessible lipid) and Ca^{2+} at a concentration ~ 50 -fold higher than the $\text{Ca}_{1/2}$ (1 mM Ca^{2+} for Syt1 C2A, 200 μM Ca^{2+} for Syt7 C2A). Increasing concentrations of NaCl were added, and the protein-to-membrane FRET was measured as described in Materials and Methods. Points and error bars shown are mean \pm standard deviation of three independent replicate measurements and are normalized based on the initial fluorescence and the final signal upon addition of EDTA.

the observed FRET signal at equilibrium, the membrane affinity of Syt1 C2A decreased steadily during the titration, with nearly complete dissociation achieved above 300 mM NaCl. This NaCl dependence of Syt1 C2A membrane binding has been reported previously by our group and others.^{12,46} By contrast, Syt7 C2A remained $\sim 80\%$ bound at 600 mM NaCl. This relative insensitivity to NaCl indicates that Syt7 C2A binds much more tightly to membranes than Syt1 C2A at high ionic strength and suggests that Syt7 C2A either has an extremely strong electrostatic attraction to the membrane or possesses an additional mechanism stabilizing its membrane-docked state.

Kinetics of C2A-Membrane Association and Dissociation. C2 domains that insert deeply into membranes with extensive hydrophobic contact, such as cPLA₂ C2, tend to associate and dissociate from membranes more slowly than domains such as Syt1 C2A and PKC α C2 possessing primarily electrostatic docking.¹² We compared the membrane association and dissociation kinetics for Syt1 C2A and Syt7 C2A on TM(-)PIP₂ membranes using stopped-flow fluorimetry. Apparent on rates were determined in the presence of saturating CaCl_2 (200 μM), which upon mixing drives full association of the domains with membrane vesicles. Off rates were measured by rapid addition of EDTA to premixed C2 domains and vesicles. As positive controls, we also measured the association and dissociation kinetics of cPLA₂ C2 and PKC α C2 domains on the same membranes. The association

and dissociation rates measured for Syt1 C2A, cPLA₂ C2, and PKC α C2 were all within 2-fold of those measured previously for the same proteins,^{7,12} with minor differences explained by the different lipid composition of the TM(-)PIP₂ membranes.

The membrane association rate of Syt7 C2A is observed to be comparable to the Syt1 C2A and PKC α C2 domains. In the presence of 100 μM total accessible lipid, Syt7 C2A binds TM(-)PIP₂ vesicles with an apparent rate constant (k_{obs}) of $157 \pm 2 \text{ s}^{-1}$ (Figure 4A and Table 3). This is 2-fold slower than

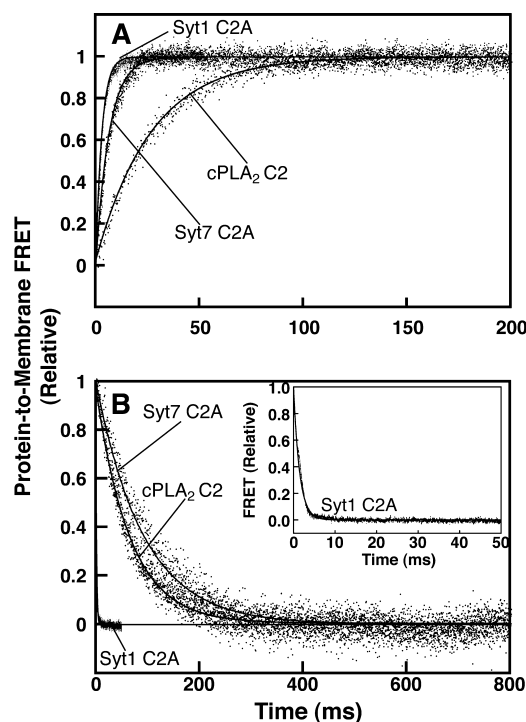


Figure 4. Kinetics of C2 domain-membrane association (A) and dissociation (B). (A) Ca^{2+} -loaded protein (0.5 μM , in buffer A + 200 μM CaCl_2) was rapidly mixed with TM(-)PIP₂ vesicles (100 μM accessible lipid; all concentrations are after mixing) in a stopped-flow fluorescence spectrometer, and dansyl fluorescence was monitored as a function of time. Data are normalized based the fits shown to single-exponential curves (solid lines, eq 2). (B) Solutions containing 0.5 μM protein, 200 μM CaCl_2 , and TM(-)PIP₂ vesicles (100 μM accessible lipid) were rapidly mixed with an equal volume of 2 mM EDTA, and protein-to-membrane FRET was observed. Fits shown are to single (eq 3, Syt7 C2A and cPLA₂ C2) or double (eq 4, Syt1 C2A) exponential decays, with rate constants given in Table 3. Inset shows an expansion of the Syt1 C2A time course.

Syt1 C2A ($340 \pm 10 \text{ s}^{-1}$) and 2-fold faster than PKC α C2 ($64 \pm 2 \text{ s}^{-1}$), both of which interact primarily with the headgroup region of membranes. All three of these domains had association curves that fit well to single-exponential equations. The association rate of Syt7 C2A was over 4-fold faster than that of cPLA₂ C2 ($37 \pm 2 \text{ s}^{-1}$, Figure 4A and Table 3). Similarly, the headgroup-binding Syt1 C2A and PKC α C2 domains associated 9-fold and 2-fold faster than cPLA₂ C2.

In contrast, the membrane dissociation rate of Syt7 C2A is vastly different from Syt1 C2A and PKC α C2 but is more similar to that of the deeply inserted cPLA₂ C2. The dissociation timecourse of Syt7 C2A following EDTA addition fits well to a single-exponential curve with a rate constant $k_{\text{off}} = 11 \pm 4 \text{ s}^{-1}$ (Figure 4B and Table 3). By contrast, Syt1 C2A requires a double-exponential fit with the major component

Table 3. Measured Rate Constants from Kinetic Experiments

protein domain	k_{off}^a (s^{-1})	k_{obs} for assocn (s^{-1})	$k_{\text{off}}/k_{\text{on}}^b$ (μM)
Syt1 C2A	670 ± 20^c	340 ± 10	41 ± 2
Syt7 C2A	11 ± 4	157 ± 2	1.5 ± 0.5
PKC α C2	50 ± 2	64 ± 2	16 ± 1
cPLA ₂ C2	15 ± 1	37 ± 2	N.D. ^d
Syt1 C2A (30% trehalose)	660 ± 10	N.D.	N.D.
Syt7 C2A (30% trehalose)	4.5 ± 0.5	N.D.	N.D.
Syt7 C2A (1.3 M Na ₂ SO ₄)	2.0 ± 0.1	N.D.	N.D.
Syt7 C2A (1.3 M NaCl)	40 ± 3	N.D.	N.D.

^aValues and errors shown are from best fits to representative data averaged over 8–12 repeat measurements for each condition. All experiments used TM(–)PIP₂ membranes. ^bValues of k_{on} were determined by dividing k_{obs} by the concentration of accessible PS (see Discussion). ^cDissociation kinetics for Syt1 C2A were biexponential. The major rate (90% of amplitude) is reported. ^dN.D.: not determined. Because cPLA₂ C2 interacts with PC rather than PS, $k_{\text{off}}/k_{\text{on}}$ is not reported for this domain.

exhibiting the off-rate constant $670 \pm 20 \text{ s}^{-1}$. The minor component was faster than the upper limit of measurement and may be a mixing artifact on this short time scale, as first-order dissociation has been reported previously for this domain.¹² cPLA₂ C2 dissociation displayed a single-exponential rate constant of $15 \pm 1 \text{ s}^{-1}$, in good agreement with a previous report.⁷ Overall, the dissociation rate of Syt7 C2A is comparable to the deeply penetrating cPLA₂ C2 domain and much slower than the headgroup binding domains Syt1 C2A and PKC α C2.

Hydrophobic Contributions to Membrane Docking.

The slow dissociation rate of Syt7 C2A is consistent with stabilization from hydrophobic membrane insertion but could also arise from other factors (see Discussion). In order to test the role of the hydrophobic effect in the slow dissociation of this domain, we measured dissociation kinetics in the presence of a kosmotropic agent, either 30% trehalose or 1.3 M Na₂SO₄. Although their precise mechanisms are unknown, these solutes generally increase the free energy penalty for water-exposed nonpolar surfaces.⁴⁷ Effects include stronger interaction between proteins and nonpolar matrices (e.g., in hydrophobic interaction chromatography), stabilized folded states of proteins, and increased membrane affinity for deeply inserting proteins such as cPLA₂ C2.^{12,48–50} The presence of either agent reduced the rate of Syt7 C2A membrane dissociation significantly (Figure 5 and Table 3). The effect of Na₂SO₄ is particularly interesting, since the ionic strength of this solution would tend to screen electrostatic interactions and weaken any electrostatic contributions to membrane binding. Indeed, inclusion of 1.3 M NaCl instead of Na₂SO₄ increased the dissociation rate (Figure 5). Inclusion of 30% trehalose decreased the Syt7 C2A dissociation rate ~2-fold but had no significant effect on the dissociation rate of Syt1 C2A (Table 3). The ionic strength sensitivity of Syt1 C2A precluded measurement in 1.3 M Na₂SO₄, since the equilibrium position of this domain in high salt is not on the membrane even in the presence of Ca²⁺ (Figure 3 and data not shown). Na₂SO₄ in the absence of Ca²⁺ was not sufficient to target Syt7 C2A to membranes, in contrast to cPLA₂ C2 (Figure S2). Overall, these results indicate that the off rate of Syt7 C2A, but not Syt1 C2A, is sensitive to the inclusion of kosmotropic solutes known

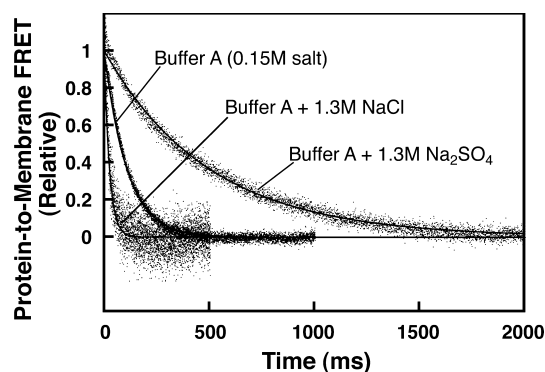


Figure 5. Effect of solutes on Syt7 C2A membrane dissociation. Dissociation was measured as described in the legend to Figure 4B, except that the indicated solutes were present in both solutions prior to mixing. Fits shown are to a single-exponential decay (eq 3), with parameters listed in Table 3.

to enhance hydrophobic components of biomolecular association.

Lack of Self-Association of Syt7 C2A. In principle, a hydrophobic contribution to protein–membrane binding could stem from several mechanisms (see Discussion). One possibility of particular interest for Syt7 C2A is protein–protein association, as this domain has been reported to self-associate in solution at high [Ca²⁺].⁵¹ In order to test for lateral self-association of membrane-bound Syt7 C2A, we measured diffusion on a supported bilayer using single-molecule total internal reflection fluorescence (TIRF) microscopy with particle tracking (Table 4 and Movies S1–S3). Alexa Fluor

Table 4. Single-Molecule Diffusion Measurements

unlabeled Syt7 C2A added (nM)	diffusion constant of fluorescent species ^a ($\mu\text{m}^2/\text{s}$)		
	AF647-Syt7C2A	AF555-PKC α C2	AF555-cPLA ₂ C2
0	1.5 ± 0.1	1.6 ± 0.1	1.5 ± 0.1
20	1.3 ± 0.1	1.5 ± 0.1	N.D.
60	0.8 ± 0.2	1.0 ± 0.1	0.9 ± 0.1

^aValues and errors shown are mean \pm SD from 3 to 6 movies of 1000 frames each and are obtained by fitting diffusion data pooled from all trajectories of each movie (600–6000 steps per movie). Measurements were taken on DOPC:DOPS (3:1) membranes at 200 μM Ca²⁺. N.D.: not determined.

647-labeled Syt7 C2A (AF647-Syt7C2A, ~5 pM) was used as a probe molecule, and either Alexa Fluor 555-labeled cPLA₂ C2 (AF555-cPLA₂C2, ~1 pM) or PKC α C2 (AF555-PKC α C2, ~3 pM) was used in the same samples as a negative control. If Syt7 C2A self-associates on the surface, then its diffusion constant should decrease upon addition of unlabeled Syt7 C2A, while diffusion of the control protein should remain constant.³³ Instead, addition of 20 nM Syt7 C2A did not change diffusion within measurement error, while 60 nM unlabeled Syt7 C2A decreased diffusion of all species by approximately the same amount (Table 4). The latter effect likely represents crowding on the membrane surface at high protein-to-lipid ratios. On the basis of the initial spot density of ~5 pM AF647-Syt7C2A, we estimate a ~1:300 protein-to-lipid ratio on the membrane after addition of 20 nM Syt7 C2A, comparable to the maximum 1:200 ratio reached in our ensemble fluorescence experiments. [We note that the cationic Syt7 C2A tends to associate strongly

with contaminants from cell lysates similarly to Syt1 C2B.⁵² The presence of these contaminants (likely nucleic acid, based on absorbance at 260 nm) gave rise to apparent self-association in some of our early experiments (data not shown), but self-association was not observed after the contaminants were removed.] Overall, these data indicate no Syt7 C2A oligomerization on the bilayer at the protein-to-lipid ratios used for the present equilibrium and kinetic measurements.

DISCUSSION

The membrane targeting mechanism of the Syt1 C2A domain has been the subject of many detailed investigations. The Syt7 C2A domain is less well characterized; it is known to exhibit a higher Ca^{2+} sensitivity of membrane docking than Syt1 C2A, but the molecular mechanisms underlying this property remain unknown. Here we report the following six new observations for Syt7 C2A docking to target membranes composed of a near-physiological lipid mixture. (i) Other anionic lipids, particularly PG, can substitute for PS equally well as a target lipid, indicating that the membrane docking mechanism includes an electrostatic component. (ii) The presence of $\text{PI}(4,5)\text{P}_2$ causes no enhancement of membrane affinity beyond that expected from nonspecific electrostatic interaction, indicating that $\text{PI}(4,5)\text{P}_2$ is not a target lipid as observed previously for Syt1 C2A.¹⁶ (iii) The Syt7 C2A–membrane interaction is stable in the presence of up to 600 mM NaCl, suggesting that the membrane docking mechanism includes an important nonelectrostatic component, in contrast to Syt1 C2A which is displaced from membranes by similar levels of salt.^{12,46} (iv) The lateral bilayer diffusion of Syt7 C2A is independent of protein concentration over a broad range of membrane surface densities, indicating that the additional membrane binding stability does not arise from surface-induced oligomerization. (v) The first direct measurement of Syt7 C2A membrane dissociation kinetics indicates they are 60-fold slower than Syt1 C2A dissociation kinetics and instead are similar to the deeply penetrating cPLA₂ C2. Unusually slow dissociation kinetics have also been reported previously for the entire cytoplasmic domain of Syt7,⁵³ and our current findings provide strong evidence that the C2A domain contributes to or dominates this behavior. (vi) The Syt1 C2A dissociation kinetics are further slowed by kosmotropic solutes, providing evidence that the rate-limiting step in dissociation may involve exposure of hydrophobic residues to solvent.

The $\text{Ca}_{1/2}$ values for Syt7 C2A binding to physiological target membranes in this study are within the range reported in previous studies using less quantitative assays with simpler lipid compositions ($1\text{--}6\ \mu\text{M}$ ^{29,54}). For comparison, recent studies reported slightly lower $\text{Ca}_{1/2}$ values of $\leq 1\ \mu\text{M}$ for membrane binding of the entire cytoplasmic region and for vesicle fusion induced by full-length Syt7.^{55,56} Thus, while the isolated C2A domain exhibits high Ca^{2+} sensitivity, it appears likely that C2B and/or interdomain interactions play additional roles in the function of full-length Syt7, analogous to recently reported interdomain cooperativity in Syt1.^{17,57–59}

The simplest Syt7 C2A membrane docking mechanism consistent with these observations is the two-step reaction illustrated in Figure 6A. In this model, the domain initially docks to its target membrane via nonspecific electrostatic attraction between the positively charged Ca^{2+} –C2 complex and anionic membrane lipids, similar to the electrostatic docking mechanism of many C2 domains including Syt1 C2A (Figure 6A, step 1). In this initial step, Ca^{2+} binding is proposed

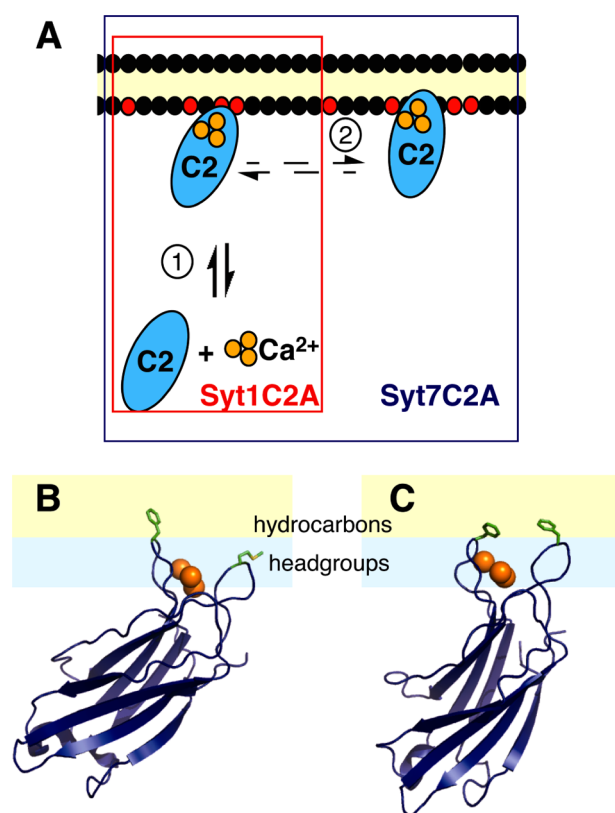


Figure 6. Model of Syt7 C2A membrane docking mechanism. (A) Proposed two-step docking model. In step 1, C2 domains interact with Ca^{2+} ions (orange circles) to drive initial electrostatic docking to membranes containing anionic lipid headgroups (red circles). Both Syt1 C2A (red box) and Syt7 C2A (blue box, inclusive of both steps) can participate in this docking event. In this model, Syt7 C2A but not Syt1 C2A can also undergo a transition to a more deeply inserted docking geometry (step 2). (B) Membrane docking geometry for Syt1 C2A previously determined through electron paramagnetic resonance (EPR) depth measurements.¹³ The published solution structure of Ca^{2+} -bound Syt1 C2A (PDB ID 1BYN⁶¹) is drawn aligned to the membrane in an illustration of the EPR-determined geometry reported by Frazier et al.¹³ The amino acid side chains of Phe234 and Met173 on the membrane-inserted Ca^{2+} binding loops are shown (green sticks). (C) Hypothesized membrane docking geometry of Syt7 C2A. The solution structure of Syt7 C2A (PDB ID 2D8K) is drawn aligned to the membrane in a manner allowing penetration of both Phe229 and Phe167 (green sticks) into the hydrocarbon interior of the membrane. For clarity in illustration, three Ca^{2+} ions are shown with the Ca^{2+} -free 2D8K structure based on their position in 1BYN after backbone alignment of the two structures. Panels B and C were created using MacPyMol.

to serve as an electrostatic switch that changes the protein–membrane electrostatic interaction from unfavorable to favorable.⁶⁰ Subsequently, the surface-bound Syt7 C2A is proposed to penetrate more deeply into the bilayer, enabling hydrophobic residues to penetrate into the hydrocarbon core (Figure 6A, step 2). Since the protein-to-membrane FRET assay employed here to observe membrane binding detects the initial electrostatic binding step, and the second membrane penetration step is unlikely to significantly alter the FRET signal further, the model adequately explains the observation that Syt7 C2A association kinetics are single-exponential and similar in rate to C2 domains with a purely electrostatic binding mechanism (Figure 4A). During the dissociation reaction, single-exponential kinetics are again observed (Figure 4B),

supporting the idea that extraction of the hydrophobic residues from the bilayer is rate-determining and slow relative to the subsequent, rapid dissociation of the electrostatic protein–membrane complex.

Published structures of the two domains offer some possible clues to the structural origin of hydrophobic enhancement for Syt7 C2A. The two C2A domains share 48% identity and 90% conserved polarity in their amino acid sequences.² Both possess two nonpolar residues that protrude from the ends of two calcium-binding loops; mutation of these in Syt1 C2A influences membrane affinity despite its predominantly electrostatic binding mechanism (Figure 6B,C).^{61,62} For Syt1 C2A these residues are Met173 and Phe234; for Syt7 C2A both hydrophobic residues are Phe (167 and 229). Since aromatic residues including Phe are known to have an unusually high affinity for the region of the bilayer hydrocarbon core adjacent to the headgroup layer, the presence of two Phe residues in Syt7 C2A may account for the stronger hydrophobic contribution to its docking mechanism.^{63,64} Figure 6C schematically shows the predicted membrane docking geometry of Syt7 C2A, with both Phe residues penetrating into the hydrocarbon layer, compared to the shallower, experimentally determined docking geometry of Syt1 C2A (Figure 6B) with just one Phe penetrating into this region.¹³ This proposed geometry of Syt7 C2A somewhat resembles that of Syt1 C2AB; Met173 penetrates into the bilayer more deeply in Syt1 C2AB than in Syt1 C2A.⁵⁹ Notably, a mutation in *Drosophila* Syt1 corresponding to F234Y diminishes secretion by 50%, suggesting membrane insertion of phenylalanine is a key determinant of protein function.⁶⁵

The proposed hydrophobic insertion of Syt7 C2A is supported by its slow dissociation kinetics and the sensitivity of the kinetics to kosmotropic agents that enhance the hydrophobic effect. Both of these features were previously observed for the cPLA₂ C2 domain, which has since been shown directly by electron paramagnetic resonance (EPR) membrane docking geometry studies to penetrate into the bilayer hydrocarbon core.^{9,12} However, further tests of the Syt7 C2A hydrophobic insertion, including future EPR docking geometry studies, are crucial since the available evidence does not fully rule out alternative models. For example, one could argue that following the electrostatic docking step, a slow conformational change occurs in the Syt7 C2A domain that buries hydrophobic residues inside the protein, rather than in the membrane. Such a conformational change appears less likely than the proposed model, given that no such rearrangement has been observed in other C2 domains, presumably due in part to the highly stable β -sandwich core of the C2 motif. Alternatively, one could argue that the kosmotrope sensitivity of Syt7 C2A dissociation reflects a protein-induced change in membrane structure, for example PS clustering or altered bilayer curvature, since kosmotrope effects on membrane dynamics are unknown. This possibility appears less likely to account for our observation of slow dissociation, since Syt1 C2AB is known to cause such clustering and bending^{18,58} but dissociates rapidly from the membrane upon removal of Ca²⁺.⁵³

The slower dissociation kinetics observed for Syt7 C2A directly account for its higher Ca²⁺ sensitivity relative to Syt1 C2A. In principle, the observed higher Ca²⁺ sensitivity for Syt7 C2A relative to Syt1 C2A could arise from either tighter Ca²⁺ binding by the free domain and/or stronger membrane affinity for the Ca²⁺-loaded domain. The latter effect has been termed target-assisted messenger affinity (TAMA).⁷ Ca²⁺ binding by

the two domains in the absence of membrane does not produce a fluorescence change (ref 12 and data not shown), and thus the intrinsic Ca²⁺ affinity is not accessible via this method. However, the membrane affinity of the Ca²⁺-loaded domains may be approximated from the ratio of the kinetic parameters k_{off} and k_{on} . Here, k_{on} can be approximated as $k_{\text{obs}}/[\text{PS}]$ since PS is the major anionic lipid target present in the TM(–)PIP₂ membranes and the protein is essentially 100% bound at equilibrium. Values of $k_{\text{off}}/k_{\text{on}}$ are shown in Table 3, with Syt7 C2A ~25-fold lower than Syt1 C2A. This represents a much tighter membrane interaction for Syt7 C2A relative to Syt1 C2A in the presence of 200 μM Ca²⁺ and could fully account for the 8-fold difference in Ca²⁺ sensitivity measured at equilibrium (Table 2). Such $k_{\text{off}}/k_{\text{on}}$ values do not correspond directly to equilibrium dissociation constants since membrane docking is accompanied by cooperative binding of multiple Ca²⁺ ions.^{16,66} Nevertheless, they show that enhanced membrane affinity of the Ca²⁺-loaded state of Syt7 C2A relative to Syt1 C2A can explain its increased Ca²⁺ sensitivity of membrane binding.

Finally, the observed differences in kinetics and Ca²⁺ sensitivity of membrane binding appear to reflect the physiological roles of the two Syt isoforms. Syt1 is the main isoform involved in rapid neurotransmitter secretion, functioning on a time scale of tens of milliseconds or less.⁶⁷ Syt7 is more broadly expressed⁵⁴ and is responsible for slower secretion of insulin in islet β cells²⁵ and glucagon in islet α cells⁶⁸ as well as lysosomal membrane fusion in macrophages and other cell types.²⁷ Furthermore, neurotransmitter secretion is triggered by peaks of intracellular [Ca²⁺] in the 100 μM range,⁶⁹ while insulin secretion is triggered by local [Ca²⁺] in the 1–10 μM range, comparable to the Ca_{1/2} of Syt7 C2A.⁷⁰ Thus, dramatically different kinetics and Ca²⁺ sensitivities of the Syt1 and Syt7 C2A domains are well tuned to the time scales and Ca²⁺ levels involved in their cellular functions.

■ ASSOCIATED CONTENT

● Supporting Information

Figures are provided showing lack of C2 domain-membrane FRET in the absence of Ca²⁺ and lack of Syt C2A domain membrane binding induced by sodium sulfate in the absence of Ca²⁺, as well as three representative movies of single-molecule diffusion. This material is available free of charge via the Internet at <http://pubs.acs.org>.

■ AUTHOR INFORMATION

Corresponding Author

*E-mail jefferson.knight@ucdenver.edu; Tel 303-556-6639; Fax 303-556-4776.

Present Address

[§]Department of Chemistry, UCLA, 607 Charles E. Young Drive East, Box 951569, Los Angeles, CA 90095-1569.

Author Contributions

[†]D.S.B. and M.D.C. contributed equally to this work.

Funding

This work was supported by NIH R01 GM-063235 to J.J.F. and by University of Colorado Denver startup funds to J.D.K.

Notes

The authors declare no competing financial interest.

ACKNOWLEDGMENTS

We thank Dr. John Corbin for help with Ca^{2+} -free protocols, Dr. Christina Leslie for providing the DNA construct for the cPLA₂ C2 domain, Dr. Linda Behlen for assistance with stopped-flow, Dr. Art Pardi for access to the Keck-funded TIRF instrument, the University of Colorado School of Pharmacy mass spectrometry facility for MALDI analysis, and Dr. Scott Reed for critically reading this manuscript.

ABBREVIATIONS

PKC, protein kinase C; Syt, synaptotagmin; TM, target membrane; PS, phosphatidylserine; PC, phosphatidylcholine; PI, phosphatidylinositol; PI(4,5)P₂ or PIP₂, phosphatidylinositol-(4,5)-bisphosphate; dPE or dansyl-PE, N-[5-(dimethylamino)naphthalene-1-sulfonyl]-1,1-dihexadecanoyl-sn-glycero-3-phosphoethanolamine; PG, phosphatidylglycerol; SNARE, soluble N-ethylmaleimide sensitive factor attachment protein receptor; GST, glutathione S-transferase; FRET, fluorescence resonance energy transfer; SUVs, sonicated unilamellar vesicles; EDTA, ethylenediaminetetraacetic acid; NTA, nitrilotriacetic acid; EPR, electron paramagnetic resonance.

REFERENCES

- (1) Martens, S. (2010) Role of C2 domain proteins during synaptic vesicle exocytosis. *Biochem. Soc. Trans.* 38, 213–216.
- (2) Nalefski, E. A., and Falke, J. J. (1996) The C2 domain calcium-binding motif: structural and functional diversity. *Protein Sci.* 5, 2375–2390.
- (3) Cho, W., and Stahelin, R. V. (2005) Membrane-protein interactions in cell signaling and membrane trafficking. *Annu. Rev. Biophys. Biomol. Struct.* 34, 119–151.
- (4) Coussens, L., Parker, P. J., Rhee, L., Yang-Feng, T. L., Chen, E., Waterfield, M. D., Francke, U., and Ullrich, A. (1986) Multiple, distinct forms of bovine and human protein kinase C suggest diversity in cellular signaling pathways. *Science* 233, 859–866.
- (5) Punta, M., Coghill, P. C., Eberhardt, R. Y., Mistry, J., Tate, J., Boursnell, C., Pang, N., Forslund, K., Ceric, G., Clements, J., Heger, A., Holm, L., Sonnhammer, E. L., Eddy, S. R., Bateman, A., and Finn, R. D. (2012) The Pfam protein families database. *Nucleic Acids Res.* 40, D290–301.
- (6) Lemmon, M. A. (2008) Membrane recognition by phospholipid-binding domains. *Nat. Rev. Mol. Cell Biol.* 9, 99–111.
- (7) Corbin, J. A., Evans, J. H., Landgraf, K. E., and Falke, J. J. (2007) Mechanism of specific membrane targeting by C2 domains: Localized pools of target lipids enhance Ca^{2+} affinity. *Biochemistry* 46, 4322–4336.
- (8) Evans, J. H., Murray, D., Leslie, C. C., and Falke, J. J. (2006) Specific translocation of protein kinase Calpha to the plasma membrane requires both Ca^{2+} and PIP₂ recognition by its C2 domain. *Mol. Biol. Cell* 17, 56–66.
- (9) Malmberg, N. J., Van Buskirk, D. R., and Falke, J. J. (2003) Membrane-docking loops of the cPLA₂ C2 domain: detailed structural analysis of the protein-membrane interface via site-directed spin-labeling. *Biochemistry* 42, 13227–13240.
- (10) Evans, J. H., Gerber, S. H., Murray, D., and Leslie, C. C. (2004) The calcium binding loops of the cytosolic phospholipase A2 C2 domain specify targeting to Golgi and ER in live cells. *Mol. Biol. Cell* 15, 371–383.
- (11) Stahelin, R. V., Rafter, J. D., Das, S., and Cho, W. (2003) The molecular basis of differential subcellular localization of C2 domains of protein kinase C-alpha and group IVa cytosolic phospholipase A2. *J. Biol. Chem.* 278, 12452–12460.
- (12) Nalefski, E. A., Wisner, M. A., Chen, J. Z., Sprang, S. R., Fukuda, M., Mikoshiba, K., and Falke, J. J. (2001) C2 domains from different

Ca^{2+} signaling pathways display functional and mechanistic diversity. *Biochemistry* 40, 3089–3100.

(13) Frazier, A. A., Roller, C. R., Havelka, J. J., Hinderliter, A., and Cafiso, D. S. (2002) Membrane-Bound Orientation and Position of the Synaptotagmin I C2A Domain by Site-Directed Spin Labeling. *Biochemistry* 42, 96–105.

(14) Radhakrishnan, A., Stein, A., Jahn, R., and Fasshauer, D. (2009) The Ca^{2+} affinity of synaptotagmin I is markedly increased by a specific interaction of its C2B domain with phosphatidylinositol 4,5-bisphosphate. *J. Biol. Chem.* 284, 25749–25760.

(15) Newton, A. C., and Keranen, L. M. (1994) Phosphatidyl-L-serine is necessary for protein kinase C's high-affinity interaction with diacylglycerol-containing membranes. *Biochemistry* 33, 6651–6658.

(16) Zhang, X., Rizo, J., and Sudhof, T. C. (1998) Mechanism of phospholipid binding by the C2A-domain of synaptotagmin I. *Biochemistry* 37, 12395–12403.

(17) Shin, O. H., Xu, J., Rizo, J., and Sudhof, T. C. (2009) Differential but convergent functions of Ca^{2+} binding to synaptotagmin-1 C2 domains mediate neurotransmitter release. *Proc. Natl. Acad. Sci. U. S. A.* 106, 16469–16474.

(18) Hui, E., Johnson, C. P., Yao, J., Dunning, F. M., and Chapman, E. R. (2009) Synaptotagmin-mediated bending of the target membrane is a critical step in Ca^{2+} -regulated fusion. *Cell* 138, 709–721.

(19) Chapman, E. R. (2008) How does synaptotagmin trigger neurotransmitter release? *Annu. Rev. Biochem.* 77, 615–641.

(20) Rizo, J., Chen, X., and Arac, D. (2006) Unraveling the mechanisms of synaptotagmin and SNARE function in neurotransmitter release. *Trends Cell Biol.* 16, 339–350.

(21) Gauthier, B. R., and Wollheim, C. B. (2008) Synaptotagmins bind calcium to release insulin. *Am. J. Physiol. Endocrinol. Metab.* 295, E1279–1286.

(22) Craxton, M. (2004) Synaptotagmin gene content of the sequenced genomes. *BMC Genomics* 5, 43.

(23) Chin, H., Choi, S. H., Jang, Y. S., Cho, S. M., Kim, H. S., Lee, J. H., Jeong, S. W., Kim, I. K., Kim, G. J., and Kwon, O. J. (2006) Protein kinase A-dependent phosphorylation of B/K protein. *Exp. Mol. Med.* 38, 144–152.

(24) Gao, Z., Reavey-Cantwell, J., Young, R. A., Jegier, P., and Wolf, B. A. (2000) Synaptotagmin III/VII isoforms mediate Ca^{2+} -induced insulin secretion in pancreatic islet beta-cells. *J. Biol. Chem.* 275, 36079–36085.

(25) Gauthier, B. R., Duhamel, D. L., Iezzi, M., Theander, S., Saltel, F., Fukuda, M., Wehrle-Haller, B., and Wollheim, C. B. (2008) Synaptotagmin VII splice variants alpha, beta, and delta are expressed in pancreatic beta-cells and regulate insulin exocytosis. *FASEB J.* 22, 194–206.

(26) Sugita, S., Han, W., Butz, S., Liu, X., Fernandez-Chacon, R., Lao, Y., and Sudhof, T. C. (2001) Synaptotagmin VII as a plasma membrane Ca^{2+} sensor in exocytosis. *Neuron* 30, 459–473.

(27) Becker, S. M., Delamarre, L., Mellman, I., and Andrews, N. W. (2009) Differential role of the Ca^{2+} sensor synaptotagmin VII in macrophages and dendritic cells. *Immunobiology* 214, 495–505.

(28) Kohout, S. C., Corbalan-Garcia, S., Torrecillas, A., Gomez-Fernandez, J. C., and Falke, J. J. (2002) C2 domains of protein kinase C isoforms alpha, beta, and gamma: activation parameters and calcium stoichiometries of the membrane-bound state. *Biochemistry* 41, 11411–11424.

(29) Sugita, S., Shin, O. H., Han, W., Lao, Y., and Sudhof, T. C. (2002) Synaptotagmins form a hierarchy of exocytotic Ca^{2+} sensors with distinct Ca^{2+} affinities. *EMBO J.* 21, 270–280.

(30) Corbin, J. A., Dirks, R. A., and Falke, J. J. (2004) GRP1 pleckstrin homology domain: Activation parameters and novel search mechanism for rare target lipid. *Biochemistry* 43, 16161–16173.

(31) Nalefski, E. A., Slazas, M. M., and Falke, J. J. (1997) Ca^{2+} -signaling cycle of a membrane-docking C2 domain. *Biochemistry* 36, 12011–12018.

- (32) Nalefski, E. A., and Falke, J. J. (2002) Use of fluorescence resonance energy transfer to monitor Ca^{2+} -triggered membrane docking of C2 domains. *Methods Mol. Biol.* 172, 295–303.
- (33) Knight, J. D., Lerner, M. G., Marcano-Velazquez, J. G., Pastor, R. W., and Falke, J. J. (2010) Single molecule diffusion of membrane-bound proteins: window into lipid contacts and bilayer dynamics. *Biophys. J.* 99, 2879–2887.
- (34) Ziemba, B. P., Knight, J. D., and Falke, J. J. (2012) Assembly of membrane-bound protein complexes: detection and analysis by single molecule diffusion. *Biochemistry* 51, 1638–1647.
- (35) Yin, J., Straight, P. D., McLoughlin, S. M., Zhou, Z., Lin, A. J., Golan, D. E., Kelleher, N. L., Kolter, R., and Walsh, C. T. (2005) Genetically encoded short peptide tag for versatile protein labeling by Sfp phosphopantetheinyl transferase. *Proc. Natl. Acad. Sci. U. S. A.* 102, 15815–15820.
- (36) Fuson, K. L., Montes, M., Robert, J. J., and Sutton, R. B. (2007) Structure of human synaptotagmin 1 C2AB in the absence of Ca^{2+} reveals a novel domain association. *Biochemistry* 46, 13041–13048.
- (37) Vrljic, M., Strop, P., Ernst, J. A., Sutton, R. B., Chu, S., and Brunger, A. T. (2010) Molecular mechanism of the synaptotagmin-SNARE interaction in Ca^{2+} -triggered vesicle fusion. *Nat. Struct. Mol. Biol.* 17, 325–331.
- (38) Herrick, D. Z., Kuo, W., Huang, H., Schwieters, C. D., Ellena, J. F., and Cafiso, D. S. (2009) Solution and Membrane-Bound Conformations of the Tandem C2A and C2B Domains of Synaptotagmin 1: Evidence for Bilayer Bridging. *J. Mol. Biol.* 390, 913–923.
- (39) Takamori, S., Holt, M., Stenius, K., Lemke, E. A., Grønborg, M., Riedel, D., Urlaub, H., Schenck, S., Brügger, B., Ringler, P., Müller, S. A., Rammner, B., Gräter, F., Hub, J. S., De Groot, B. L., Mieskes, G., Moriyama, Y., Klingauf, J., Grubmüller, H., Heuser, J., Wieland, F., and Jahn, R. (2006) Molecular anatomy of a trafficking organelle. *Cell* 127, 831–846.
- (40) Voelker, D. R. (2008) Lipid assembly into cell membranes, in *Biochemistry of Lipids, Lipoproteins and Membranes* (Vance, D. E., and Vance, J. E., Eds.) 5th ed., pp 441–484, Elsevier, Amsterdam.
- (41) Paterson, J. K., Renkema, K., Burden, L., Halleck, M. S., Schlegel, R. A., Williamson, P., and Daleke, D. L. (2006) Lipid specific activation of the murine P4-ATPase Atp8a1 (ATPase II). *Biochemistry* 45, 5367–5376.
- (42) van Meer, G., Voelker, D. R., and Feigenson, G. W. (2008) Membrane lipids: where they are and how they behave. *Nat. Rev. Mol. Cell Biol.* 9, 112–124.
- (43) Di Paolo, G., and De Camilli, P. (2006) Phosphoinositides in cell regulation and membrane dynamics. *Nature* 443, 651–657.
- (44) Tucker, W. C., Edwardson, J. M., Bai, J., Kim, H. J., Martin, T. F., and Chapman, E. R. (2003) Identification of synaptotagmin effectors via acute inhibition of secretion from cracked PC12 cells. *J. Cell Biol.* 162, 199–209.
- (45) Corbalan-Garcia, S., Garcia-Garcia, J., Rodriguez-Alfaro, J. A., and Gomez-Fernandez, J. C. (2003) A new phosphatidylinositol 4,5-bisphosphate-binding site located in the C2 domain of protein kinase Calpha. *J. Biol. Chem.* 278, 4972–4980.
- (46) Hui, E., Bai, J., and Chapman, E. R. (2006) Ca^{2+} -triggered simultaneous membrane penetration of the tandem C2-domains of synaptotagmin I. *Biophys. J.* 91, 1767–1777.
- (47) Creighton, T. E. (1993) *Proteins: Structures and Molecular Properties*, 2nd ed., Freeman, New York, p 156.
- (48) Queiroz, J. A., Tomaz, C. T., and Cabral, J. M. (2001) Hydrophobic interaction chromatography of proteins. *J. Biotechnol.* 87, 143–159.
- (49) Jain, N. K., and Roy, I. (2009) Effect of trehalose on protein structure. *Protein Sci.* 18, 24–36.
- (50) Nalefski, E. A., McDonagh, T., Somers, W., Seehra, J., Falke, J. J., and Clark, J. D. (1998) Independent folding and ligand specificity of the C2 calcium-dependent lipid binding domain of cytosolic phospholipase A2. *J. Biol. Chem.* 273, 1365–1372.
- (51) Fukuda, M., and Mikoshiba, K. (2001) Mechanism of the calcium-dependent multimerization of synaptotagmin VII mediated by its first and second C2 domains. *J. Biol. Chem.* 276, 27670–27676.
- (52) Ubach, J., Lao, Y., Fernandez, I., Arac, D., Sudhof, T. C., and Rizo, J. (2001) The C2B domain of synaptotagmin I is a Ca^{2+} -binding module. *Biochemistry* 40, 5854–5860.
- (53) Hui, E., Bai, J., Wang, P., Sugimori, M., Llinas, R. R., and Chapman, E. R. (2005) Three distinct kinetic groupings of the synaptotagmin family: candidate sensors for rapid and delayed exocytosis. *Proc. Natl. Acad. Sci. U. S. A.* 102, 5210–5214.
- (54) Li, C., Ullrich, B., Zhang, J. Z., Anderson, R. G., Brose, N., and Sudhof, T. C. (1995) Ca^{2+} -dependent and -independent activities of neural and non-neural synaptotagmins. *Nature* 375, 594–599.
- (55) Wang, P., Chicka, M. C., Bhalla, A., Richards, D. A., and Chapman, E. R. (2005) Synaptotagmin VII is targeted to secretory organelles in PC12 cells, where it functions as a high-affinity calcium sensor. *Mol. Cell. Biol.* 25, 8693–8702.
- (56) Zhang, Z., Wu, Y., Wang, Z., Dunning, F. M., Rehfsuss, J., Ramanan, D., Chapman, E. R., and Jackson, M. B. (2011) Release mode of large and small dense-core vesicles specified by different synaptotagmin isoforms in PC12 cells. *Mol. Biol. Cell* 22, 2324–2336.
- (57) Vrljic, M., Strop, P., Hill, R. C., Hansen, K. C., Chu, S., and Brunger, A. T. (2011) Post-translational modifications and lipid binding profile of insect cell-expressed full-length mammalian synaptotagmin 1. *Biochemistry* 50, 9998–10012.
- (58) Lai, A. L., Tamm, L. K., Ellena, J. F., and Cafiso, D. S. (2011) Synaptotagmin 1 modulates lipid acyl chain order in lipid bilayers by demixing phosphatidylserine. *J. Biol. Chem.* 286, 25291–25300.
- (59) Herrick, D. Z., Sterbling, S., Rasch, K. A., Hinderliter, A., and Cafiso, D. S. (2006) Position of synaptotagmin I at the membrane interface: cooperative interactions of tandem C2 domains. *Biochemistry* 45, 9668–9674.
- (60) Murray, D., and Honig, B. (2002) Electrostatic control of the membrane targeting of C2 domains. *Mol. Cell* 9, 145–154.
- (61) Shao, X., Fernandez, I., Sudhof, T. C., and Rizo, J. (1998) Solution structures of the Ca^{2+} -free and Ca^{2+} -bound C2A domain of synaptotagmin I: does Ca^{2+} induce a conformational change? *Biochemistry* 37, 16106–16115.
- (62) Gerber, S. H., Rizo, J., and Sudhof, T. C. (2002) Role of electrostatic and hydrophobic interactions in Ca^{2+} -dependent phospholipid binding by the C(2)A-domain from synaptotagmin I. *Diabetes* 51 (Suppl. 1), S12–18.
- (63) Wimley, W. C., and White, S. H. (1996) Experimentally determined hydrophobicity scale for proteins at membrane interfaces. *Nat. Struct. Biol.* 3, 842–848.
- (64) Hong, H., Park, S., Jimenez, R. H., Rinehart, D., and Tamm, L. K. (2007) Role of aromatic side chains in the folding and thermodynamic stability of integral membrane proteins. *J. Am. Chem. Soc.* 129, 8320–8327.
- (65) Paddock, B. E., Wang, Z., Biela, L. M., Chen, K., Getzy, M. D., Striegel, A., Richmond, J. E., Chapman, E. R., Featherstone, D. E., and Reist, N. E. (2011) Membrane penetration by synaptotagmin is required for coupling calcium binding to vesicle fusion in vivo. *J. Neurosci.* 31, 2248–2257.
- (66) Kertz, J. A., Almeida, P. F., Frazier, A. A., Berg, A. K., and Hinderliter, A. (2007) The cooperative response of synaptotagmin I C2A. A hypothesis for a Ca^{2+} -driven molecular hammer. *Biophys. J.* 92, 1409–1418.
- (67) Heidelberger, R., Heinemann, C., Neher, E., and Matthews, G. (1994) Calcium dependence of the rate of exocytosis in a synaptic terminal. *Nature* 371, 513–515.
- (68) Gustavsson, N., Wei, S. H., Hoang, D. N., Lao, Y., Zhang, Q., Radda, G. K., Rorsman, P., Sudhof, T. C., and Han, W. (2009) Synaptotagmin-7 is a principal Ca^{2+} sensor for Ca^{2+} -induced glucagon exocytosis in pancreas. *J. Physiol.* 587, 1169–1178.
- (69) Llinas, R., Sugimori, M., and Silver, R. B. (1992) Microdomains of high calcium concentration in a presynaptic terminal. *Science* 256, 677–679.

(70) Quesada, I., Martin, F., and Soria, B. (2000) Nutrient modulation of polarized and sustained submembrane Ca^{2+} microgradients in mouse pancreatic islet cells. *J. Physiol.* 525 (Pt 1), 159–167.